Title

Response of anaerobic methanotrophs and benthic foraminifera to 20 years of methane emission from a gas blowout in the North Sea

Authors

Wilfert, Philipp
Krause, Stefan
Liebetrau, Volker
et al.

Publication Date

2015-12-01

DOI

10.1016/j.marpetgeo.2015.07.012

Peer reviewed

Marine and Petroleum Geology 68 (2015) 731–742

Contents lists available at ScienceDirect

Marine and Petroleum Geology

journal homepage: www.elsevier.com/locate/marpetgeo

Response of anaerobic methanotrophs and benthic foraminifera to 20 years of methane emission from a gas blowout in the North Sea

Philipp Wilfert**, Stefan Krause, Volker Liebetrau, Joachim Schönfeld, Matthias Haeckel, Peter Linke, Tina Treude*

GEOMAR Helmholtz Centre for Ocean Research Kiel, Department of Marine Biogeochemistry, Wischhofstr. 1-3, 24148 Kiel, Germany

ARTICLE INFO

Article history:
Received 20 December 2013
Received in revised form 1 December 2014
Accepted 10 July 2015
Available online 17 July 2015

Keywords:
AOM
Sulfate reduction
Cold seep
Authigenic carbonates
Carbon isotopes

ABSTRACT

Methane emissions from marine sediments are partly controlled by microbial anaerobic oxidation of methane (AOM). AOM provides a long-term sink for carbon through precipitation of methane-derived authigenic carbonates (MDAC). Estimates on the adaptation time of this benthic methane filter as well as on the establishment of related processes and communities after an onset of methane seepage are rare. In the North Sea, considerable amounts of methane have been released since 20 years from a man-made gas blowout offering an ideal natural laboratory to study the effects of methane seepage on initially "pristine" sediment. Sediment cores were taken from the blowout crater and a reference site (50 m distance) in 2011 and 2012, respectively, to investigate porewater chemistry, the AOM community and activity, the presence of authigenic carbonates, and benthic foraminiferal assemblages. Potential AOM activity (up to 3060 nmol cm^{-3} sediment d^{-1} or 375 mmol m^{-2} d^{-1}) was detected only in the blowout crater up to the maximum sampling depth of 18 cm. CARD-FISH analyzes suggest that monospecific ANME-2 aggregates were the only type of AOM organisms present, showing densities (up to $2.2*10^7$ aggregates cm^{-3}) similar to established methane seeps. No evidence for recent MDAC formation was found using stable isotope analyzes ($\delta^{13}C$ and $\delta^{18}O$). In contrast, the carbon isotopic signature of methane was recorded by the epibenthic foraminifer *Cibicides lobatulus* ($\delta^{13}C$ −0.66‰). Surprisingly, the foraminiferal assemblage in the blowout crater was dominated by *Cibicides* and other species commonly found in the Norwegian Channel and fjords, indicating that these organisms have responded sensitively to the specific environmental conditions at the blowout. The high activity and abundance of AOM organisms only at the blowout site suggests adaptation to a strong increase in methane flux in the order of at most two decades. High gas discharge dynamics in permeable surface sediments facilitate fast sulfate replenishing and stimulation of AOM. The accompanied prevention of total alkalinity build-up in the porewater thereby appears to inhibit the formation of substantial methane-derived authigenic carbonate at least within the given time window.

1. Introduction

The Global Warming potential of methane (CH_4) is about 25 times higher compared to carbon dioxide (IPCC, 2007). In the oceans, methane emissions from seafloor sources are partly controlled by sulfate-dependent anaerobic oxidation of methane (AOM) (Knittel and Boetius, 2009). AOM is mediated by anaerobic methanotrophic archaea (ANME) (Milucka et al., 2012) or by different types of microbial consortia involving both ANME and sulfate-reducing bacteria (Boetius et al., 2000; Orphan et al., 2001; Knittel et al., 2005). During AOM, methane is oxidized using sulfate (SO_4^{2-}) as terminal electron acceptor. End-products of AOM are bicarbonate (HCO_3^-), water (H_2O) and sulfide (HS^-) (Barnes and Goldberg, 1976, Equation (1)):

$$CH_4 + SO_4^{2-} \rightarrow HCO_3^- + HS^- + H_2O \quad (1)$$

* Corresponding author. Present address: University of California Los Angeles, Department of Earth, Planetary and Space Sciences, Department of Atmospheric and Oceanic Sciences, 595 Charles E. Young Drive East, Los Angeles, CA 90095-1567, USA.
** Corresponding author. Present address: Wetsus – Centre of Excellence for Sustainable Water Technology, Agora 1, Leeuwarden, The Netherlands.
E-mail addresses: philipp.wilfert@wetsus.nl (P. Wilfert), ttreude@g.ucla.edu (T. Treude).

http://dx.doi.org/10.1016/j.marpetgeo.2015.07.012
0264-8172/

AOM is commonly found within the sulfate–methane transition zone (SMTZ) of sediments (Jørgensen et al., 1990; Treude et al., 2005c). Highest abundances of AOM organisms and methane turnover rates are reported from cold seep ecosystems (e.g., Treude et al., 2003; Knittel et al., 2005; Niemann et al., 2006; Sommer et al., 2010; Krause et al., 2013), where methane-loaded fluids or free gas ascend to the sediment surface. In these advective systems, AOM is often confined to a narrow SMTZ in the top 10 cm of the sediment (Treude et al., 2003; Knittel and Boetius, 2009). Depending on the advective fluid and methane flux, AOM consumes between 0 and 100% of the methane before it enters the water column (Treude et al., 2003; Niemann et al., 2006; Knittel and Boetius, 2009).

The reaction of AOM leads to an increase in porewater alkalinity via the formation of bicarbonate and thereby induces the precipitation of methane-derived authigenic carbonates (MDAC; Peckmann et al., 2001), which represents a durable sink for the carbon. Vast MDAC deposits, embedded in near-surface sediments, are reported from cold seeps (e.g., Ritger et al., 1987; Bohrmann et al., 1998; Peckmann et al., 2001; Greinert et al., 2001; Aloisi et al., 2002; Niemann et al., 2005; Liebetrau et al., 2010). Since the methane emanating at these seeps is often of biogenic origin, and therefore depleted in the heavier ^{13}C carbon isotope, MDAC also bear a light carbon isotope signature (Schoell, 1988; Peckmann et al., 1999; Thiel et al., 2001). Thus, MDAC can be distinguished from other marine carbonates by its isotope composition. Shells of biomineralizing organisms living at cold seeps carry a clear methane-derived carbon isotopic signature if their metabolism relies on methanotrophic processes or methane-related food sources (e.g. McConnaughey et al., 1997; Hein et al., 2006). If, however, carbon used for biomineralization is derived from ambient seawater, isotope classification is less distinct. For example, living benthic foraminifera often showed no profound negative offset in $\delta^{13}C$ values of their calcareous shell material under the influence of methane seepage (Rathburn et al., 2000; Stott et al., 2002; Torres, 2003; Hill et al., 2004; Panieri, 2006). There is growing evidence, however, that single specimens exhibit a wider range in $\delta^{13}C$ values than at control sites. Once foraminifera are dwelling in mats of the sulfur-oxidizing bacteria *Beggiatoa*, foraminiferal cytoplasm and shell carbon isotopes are altered by the highly negative methane signal (Rathburn et al., 2003; Hill et al., 2004; Panieri, 2006). Only at the Håkon-Mosby mud volcano, a seepage structure with extensive fluid and methane discharge, a consistent negative shift in epibenthic foraminiferal $\delta^{13}C$ values was detected (Mackensen et al., 2006). Detailed investigations on diet and assemblage composition of benthic foraminifera in combination with carbon isotopic analyzes may therefore provide an important tool to study the impact of methane emissions on benthic cold-seep communities.

Here, we present a combined investigation of AOM activity, MDAC, and benthic foraminiferal communities from a man-made gas blowout site in the North Sea, where large quantities of methane have been released into the hydrosphere for more than 20 years (Schneider von Deimling et al., in this issue). In particular, this site offers a natural laboratory to study the response time of the benthic methanotrophic community to a new methane seepage event, the potential of sediments to form a long-term sink of methane-derived carbon, and the impact of methane venting on benthic foraminiferal assemblages and their stable isotope composition.

2. Materials and methods

2.1. Study site and sediment sampling

In 1990, an exploration well (UK22/4b) penetrated a shallow methane pocket, causing a gas blowout in the northern North Sea (~57°55.41′N; 001°37.95′E; Rehder et al., 1998) and forming a crater (depth: 20 m, diameter: ca. 60 m, Fig. 1) on the seafloor (Schneider von Deimling et al., 2007; Schneider von Deimling et al., in this issue). Biogenic methane ($\delta^{13}C$ about −75‰, Leifer et al. in this issue; Schneider von Deimling et al. in this issue) is vigorously and continuously emitted until the present (Leifer and Judd, in this issue).

Three sediment push cores (length: 18 cm) were taken inside the blowout crater at 118 m water depth using a Triton XLS work class ROV on board of the survey vessel NOORDHOEK PATHFINDER in September 2011 (Fig. 1). Two additional push cores (length: 15 cm) were taken at a reference site, 50 m south-east of the crater at 99 m water depth in July 2012, using the Schilling work-class ROV KIEL 6000 during cruise CE12010 with RV CELTIC EXPLORER (Linke, 2012, Fig. 1). One of the cores from each site was used to study porewater chemistry. The other core was used to study the activity and abundance of the AOM community and to extract clam shells and rock fragments for isotope analyzes. The additional third core, which was taken only from the crater, was used to study the benthic foraminiferal assemblage and their carbon and oxygen isotope signatures. In addition to sediment coring, samples (clam

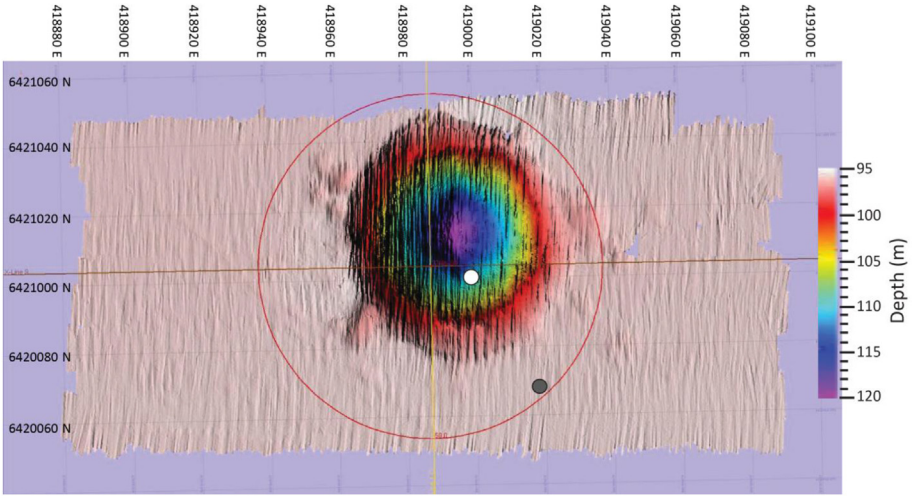

Fig. 1. Bathymetric map obtained during the NOORDHOEK PATHFINDER cruise showing the sampling position in the blowout crater (white dot) and at the reference site (grey dot). The circle with a radius of 50 m represents a scale.

shells, cemented sediment and rock fragments) for the identification of MDAC were collected from surface sediments by the submersible JAGO during RV ALKOR cruise AL290. These samples were transferred from the sediment to the sample container of the submersible using a hydraulic manipulator arm. All sampling stations and measured parameters are summarized in Table 1.

2.2. Porewater chemistry

Cores were sectioned in 1–2 cm intervals and porewater was extracted from the sediment using a low pressure-squeezer (5 bar) equipped with 0.2 μm filters. Porewater sulfate concentrations were determined by ion-chromatography, total alkalinity by titration of samples with 0.02 N HCl, and porosity by weight difference before and after freeze-drying of the sediment assuming a sediment density of 2.5 g cm^{-3} and a porewater density of 1.023 g cm^{-3}. For details on the employed methods as well as analytical precisions see Haffert et al. (2013).

2.3. Potential AOM activity

One core of each site was sectioned into three horizons of 0–6, 6–12, and 12–18 (blowout crater) and 0–6, 6–12, and 12–15 (reference site) cm below surface (cmbsf) to study the activity and abundance of AOM organisms. Analyzes of AOM activity were conducted under anoxic conditions using the Hungate method (Hungate, 1950) or in an anoxic acrylic glove box (Innovative Technologies Inc., Amesbury, MA, USA). Potential AOM activity, i.e., the maximum AOM capacity under non-limiting sulfate and saturated (atmospheric pressure) methane concentrations, was determined in in-vitro time-series experiments using sediment slurries according to Nauhaus et al. (2002) by following the accumulation of AOM end-products sulfide and total alkalinity. For preparation of final slurries (dilution 1:8), first, stock slurries were prepared by diluting sediments (1:2) with artificial seawater medium for sulfate-reducing bacteria (Widdel and Bak, 1992). Stock slurries were pre-incubated with a methane (purity grade >99.995%) headspace (p_{CH_4} = 1.1 bar, 91 days, 13 °C, in the dark). After pre-incubation, slurries were transferred into Hungate tubes (17 mL), diluted with seawater medium (1:8) and incubated with a methane (purity grade >99.995%) headspace for the determination of gross (=methane-independent and methane-dependent) sulfate reduction rates, or with a N_2 headspace for the determination of methane-independent sulfate reduction rates ($p_{CH_4\ respectively\ N_2}$ = 1.1 bar, incubation time = 47 days, in the dark). Incubations were conducted at different temperatures (4, 13, 20, 37 and 60 °C, n = 3 per depth horizon) in replicate set ups to identify the temperature optimum for AOM in blowout crater sediments. Twice a week, samples (100 and 50 μL, respectively), were taken from the clear supernatant of the Hungate tubes to determine sulfide concentrations (Cord-Ruwisch, 1985) and total alkalinity (Ivanenkov and Lyakhin, 1978). Potential methane-dependent sulfate reduction (=AOM) rates were calculated by subtracting methane independent (=organoclastic) sulfate reduction from gross sulfate reduction rates. Samples for measuring AOM activity in sediments from the reference site were treated analogue to samples from the blowout crater. However, the activity was determined at 13 °C only.

Additionally, after confirming AOM activity in the sediments from the blowout crater during the time-series experiment (see above), radiotracer experiments were conducted in the same slurries at 13 °C only. About 90 days after starting the time-series incubations, part of the medium was exchanged in the 17 mL Hungate tubes to reduce the sulfide level and to re-establish the initial dilution (1:8). Then slurries were transferred into smaller, CH_4-flushed Hungate tubes (5 mL). Due to a lack of material, samples had to be further diluted (final dilution: 1:10 or 1:11). Then radiolabelled sulfate (175 kBq $^{35}SO_4^{2-}$ dissolved in 8 μL sterile water, specific activity 37 TBq mmol L^{-1}) or methane (10 kBq $^{14}CH_4$ dissolved in 30 μL anoxic sterile water, specific activity 2.28 GBq mmol L^{-1}) was injected into the Hungate tubes (n = 3 per depth horizon) through rubber stoppers. The incubation (24 h, 13 °C, in the dark) was terminated by transferring sediment slurries into 20 mL 2.5% (w/w) NaOH for AOM and into 20 mL 20% (w/w) zinc acetate for sulfate reduction, respectively, and shaken vigorously. Controls (n = 5 for AOM and n = 3 for sulfate reduction rate measurements) were treated identically to the samples but were terminated before radiotracer injection. Rates of sulfate reduction were determined using the cold-chromium distillation method (Kallmeyer et al., 2004). AOM rates were determined by gas chromatography and $^{14}CH_4$ combustion (Treude et al., 2005b) and $^{14}CO_2$ acidification/trapping (Joye et al., 2004).

2.4. CARD-FISH

From each sediment horizon (see 2.3), 0.5 cm^3 sediment was fixed (3 h) with 1.5 mL formaldehyde (3%), washed three times with phosphate buffered saline (PBS; centrifuged at 4500 g, 10 min, 4 °C) and stored in PBS/EtOH (1:1) at −20 °C. Fixed samples were diluted (1:1000) with PBS and sonicated (amplitude 20% (40 W), 2 × 20 s, cycle 20%). Aliquots of 1000 μL were filtered on 0.2 μm polycarbonate filters and embedded in agarose.

Catalyzed Reporter Deposition Fluorescence In Situ Hybridization (CARD-FISH) was performed to identify and quantify AOM organisms (Pernthaler et al., 2002) using probes ANME-1-350 (Boetius et al., 2000), ANME-2-538 (Treude et al., 2005a), ANME-3-1249 (Lösekann et al., 2007) and EUB-338 (Amann et al., 1990). Biotin-labeled oligonucleotide probes were purchased from Biomers (Ulm, Germany). Binding of streptavidin-HRP to probes and tyramide signal amplification was realized using the TSA™ Kit #22 with HRP-streptavidin and Alexa Flour® 488 tyramide according to the manufacturer's instructions (Invitrogen, Karlsruhe). Formamide concentrations were applied according to published values (see respective probe citations above). Hybridized filters were counter stained with 4′,6-Diamidin-2-phenylindol (DAPI). Aggregate counting was performed using epifluorescence microscopy.

Table 1
List of stations and parameters measured.

Cruise year	Sampling device	Area	Latitude (N)	Longitude (E)	Water depth (m)	PW	Foram	MDAC	AOM
AL290 2006	JAGO 952	22/4b Crater	57°55.290′	01°37.860′	119			X	
NP 2011	ROV10 PC33	22/4b Crater	57°55.360′	01°37.862′	118	X			
NP 2011	ROV10 PC36	22/4b Crater	57°55.360′	01°37.862′	118		X		
NP 2011	ROV10 PC35	22/4b Crater	57°55.360′	01°37.862′	118			X	X
CE12010 2012	ROV9 PC35	22/4b Ref.	57°55.270′	01°37.888′	99.4	X			
CE12010 2012	ROV9 PC52	22/4b Ref.	57°55.270′	01°37.888′	99.4				X

Abbreviations: AL = RV Alkor, CE = RV Celtic Explorer, NP = Nordhoek Pathfinder.

2.5. Carbonate analyzes

For carbonate analyzes we used clam shells, and cemented sediment collected either from sediment cores or from surface sediments in the blowout crater. All samples were examined for overgrowth of authigenic carbonates using a dissecting microscope. Once petrographic evidences for post-depositional carbonate precipitation were recognized (Fig. 2), material was extracted using a hand-held dental driller. Samples were further analyzed for their mineralogy (between 2 and 70 2θ using a Philips X-ray diffractometer PW 1710 with monochromatic CoKα; spectra were analyzed using XPowder®) and for their stable oxygen and carbon composition using a Thermo Fisher Scientific 253 Mass Spectrometer coupled to a CARBO KIEL online carbonate preparation line (^{18}O and δ^{13}C values are referred to the VPDB scale).

2.6. Foraminifera

The uppermost 1 cm sediment of the core used for foraminiferal studies was carefully sliced off and preserved with rose Bengal solution (2 g Bengal per liter 98% ethanol). The sample was prepared and analyzed for living and dead benthic foraminifera and their assemblage composition following the Foraminiferal Biomonitoring (FOBIMO) protocol (Schönfeld et al., 2012). Selected species were documented with a Keyence VHX – 700 FD digital camera. About 2–4 living, well-stained specimens of *Cibicides lobatulus* with glossy and transparent chamber walls were picked from the grain size fraction >125 μm and analyzed for their stable isotope composition by mass spectrometry (see 2.5). The standard deviation of eight replicate measurements of an internal carbonate standard referenced to NBS 19 was 0.04‰ for δ^{18}O and 0.03‰ for δ^{13}C for this sample set.

3. Results

3.1. Porosity and porewater profiles

Porosity in sediments from the blowout crater was slightly higher (0.49–0.52) compared to the reference sediments (0.36–0.44) and did not show any considerable decrease with depth (Fig. 3). Total alkalinity in blowout sediments increased linear from 3.5 to 5.5 meq L^{-1} in the top 4 cm, below total alkalinity varied between 4.1 and 5.2 meq L^{-1} (Fig. 3). At the reference site, total alkalinity was lower and more constant with depth (2.3–3.0 meq L^{-1}). Sulfate concentrations in crater sediments decreased slightly from 29 mmol L^{-1} at the sediment–water interface to 25 mmol L^{-1} at 15 cmbsf (Fig. 3). In the reference core, sulfate concentrations were constant at 29–30 mmol L^{-1}.

3.2. Potential AOM rates

In the temperature-dependent time-series experiments, highest potential methane-dependent sulfate reduction rates (=potential AOM) were detected at 13 and 20 °C (Fig. 4), indicating the presence of psychrophilic to mesophilic microorganisms. Methanotrophic organisms were probably adapted to the relatively constant in-situ temperatures (7–10 °C) in the lower water column of the study site (Nauw et al., in this issue). AOM activity was below detection limit at 37 and 60 °C. In the following, we will concentrate on AOM activity determined at 13 °C, i.e., within the detected temperature optimum. Methane-independent (=organoclastic) sulfate reduction activity determined at 13 °C via sulfide and total alkalinity production in methane-free sediment slurries from all sediment horizons of the blowout crater core was detectable in only 6 out of 18 samples (2 methods × 3 horizons × 3 replicates = 18 samples; data not shown). Four out of these six active samples featured rates below 150 nm cm^{-3} d^{-1}; only two samples peaked with rates up to 540 nmol cm^{-3} d^{-1}. In comparison, sulfate reduction rates in samples incubated at 13 °C with methane were between 1100 and 3130 nmol cm^{-3} d^{-1}. The derived AOM rates at 13 °C ranged between 1000 and 3060 nmol cm^{-3} d^{-1} (Fig. 5). AOM rates determined via sulfide production were about 1.3 higher compared to rates determined via total alkalinity production (Fig. 5). Both methods risk underestimation of AOM by precipitation of either metal sulfides or authigenic carbonates, respectively. A slight decrease of total alkalinity in sediment slurries incubated at 60 °C (data not shown) indicated temperature-controlled carbonate precipitation.

In radiotracer experiments at 13 °C with either ^{14}C-methane or ^{35}S-sulfate, AOM activity was 90% of sulfate reduction in the central horizon (6–12 cmbsf) or even exceeded it by 5 and 14% in the top (0–6 cmbsf) and bottom (12–18 cmbsf) horizons, respectively (data not shown). Generally, incubations with radiotracers generated the lowest AOM rates (Fig. 5), for which we have no coherent explanation. In previous studies, in-vitro radiotracer and in-vitro time-series determinations of AOM rates in seep sediments agreed well (compare Nauhaus et al., 2002; Treude et al., 2003). Perhaps higher dilution (1:11 and 1:10 compared to 1:8) of the sediments or fast depletion of methane in the headspace-free Hungate tubes had negative effects on AOM activity in the radiotracer experiment. Irrespective of discrepancies between the absolute rates, all three methods revealed similar distribution patterns of AOM activity in blowout crater sediments. AOM rates were highest in the deepest horizon (12–18 cmbsf) followed by the upper (0–6 cmbsf) and intermediate (6–12 cmbsf) horizons (Fig. 5). The integrated AOM rate (0–18 cmbsf), calculated from the increase of sulfide over time, was 375 mmol d^{-1} m^{-2}. No increase in total alkalinity or sulfide was detected in methane-free and methane-amended samples from the

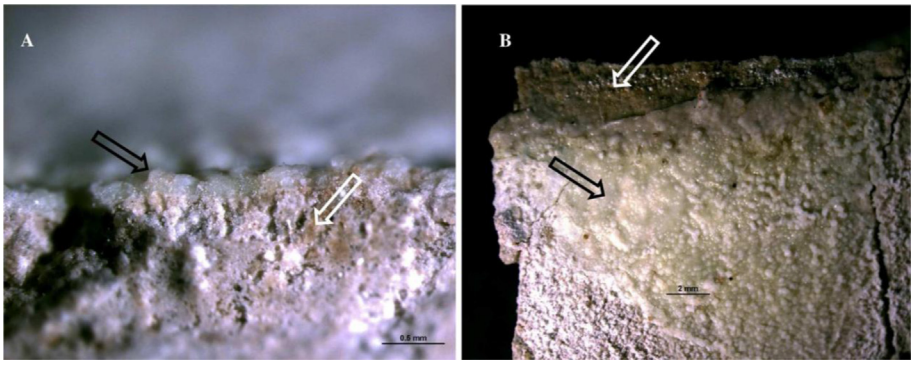

Fig. 2. Cross-section (A) and top view (B) of sediment samples from the blowout crater showing bulk sediment (white arrows) covered with crystalline structures resembling carbonate crusts (black arrows).

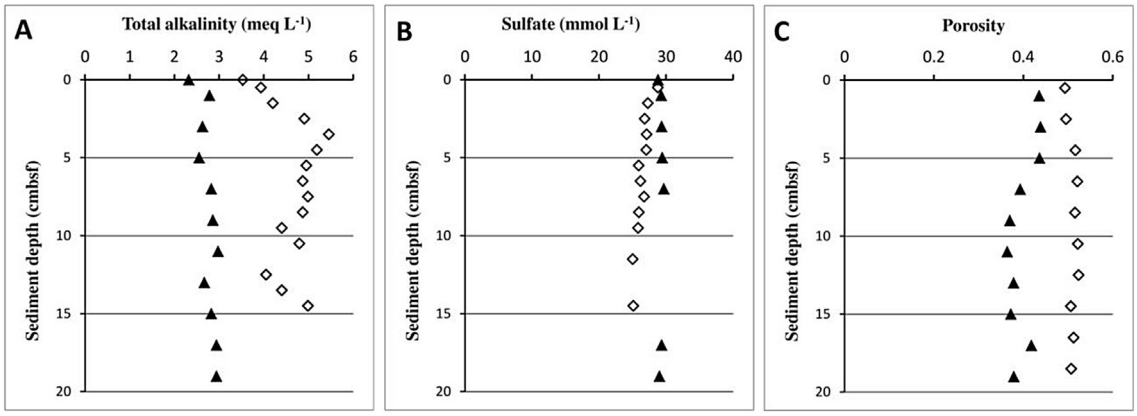

Fig. 3. Biogeochemical profiles of sediments at the blowout crater (◊) and at the reference site, 50 m away from the crater (▲): (A) total alkalinity, (B) sulfate concentration, (C) porosity.

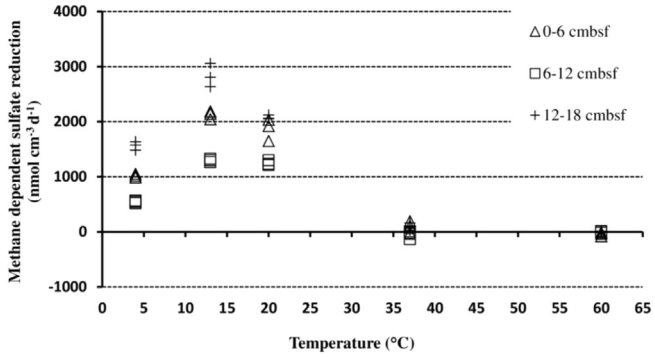

Fig. 4. Potential methane-dependent sulfate reduction rates (=potential AOM) determined in vitro by measuring the increase of sulfide concentrations with and without methane addition at different temperatures over 47 days. Symbols represent different sediment horizons. Per horizon, three replicates are shown. The pattern was similar for determinations via the increase of total alkalinity (data not shown).

reference site over the entire incubation time (47 d), indicating that AOM activity was either absent or negligible.

3.3. CARD-FISH

In all three horizons of the blowout crater sediments (0–6, 6–12, 12–18 cmbsf), high abundances of aggregates consisting of coccoid cells with an average cell diameter of 0.7 ± 0.02 μm (95% CI, n = 117) were detected with the ANME-2 probe (Fig. 6).

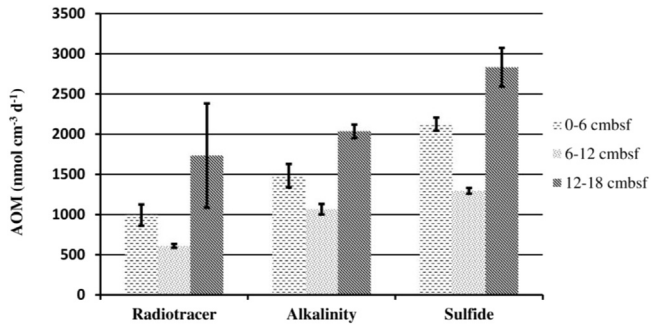

Fig. 5. Mean potential AOM rates in blowout sediments (0–6, 6–12, 12–18 cm sediment depth) determined in vitro via radiotracer techniques, total alkalinity increase, or increase in dissolved sulfide concentration (incubation temperature 13 °C; n = 3, bars indicate 95% CI).

Mean diameters of cell aggregates ranged between 3 ± 0.4 and 4 ± 0.6 μm in the upper and deepest horizon respectively (95% CI, n = 25). The aggregates appeared to be monospecific since no cells besides ANME-2 were visible in DAPI counter stainings. Furthermore, no aggregate cells were detected by Eubacteria (EUB), ANME-1 or ANME-3 probes. We therefore assumed that all aggregates consisted of ANME-2 cells and conducted aggregate counts only with DAPI-stained samples. Highest density of DAPI-stained aggregates was found in the shallowest sediment horizon, which was twice as high as in the deepest horizon and almost four times higher than in the intermediate horizon. Integrating the aggregate counts over 0–18 cmbsf equaled $2.5*10^{12}$ aggregates m^{-2}. No aggregates were found in the reference sediment, while abundance of single cells was similar between crater and reference sediment (Table 2).

3.4. Carbonate composition

In first summary, detailed visual ROV and JAGO based inspection of the blowout crater showed no clear evidence for substantial authigenic carbonate precipitation, when compared to structures known from long lasting natural induced seep systems of different settings (Teichert et al., 2003; Bayon et al., 2009; Liebetrau et al., 2010). Nevertheless, some carbonate-like samples were recovered from sediments of the crater bottom and their mineralogical inventory and stable isotope composition ($\delta^{13}C$ and $\delta^{18}O$) was analyzed to test for a potential methane-related origin (Table 3). Small-scale (mm to cm) crystalline structures, extracted from a crack and from top of the sediment (Fig. 2), mainly consisted of brucite ($Mg(OH)_2$), polymorphs of calcium carbonate (calcite and aragonite, $CaCO_3$) and magnesite ($MgCO_3$). Subsamples of a vein-like filling of a crack in solidified or cemented sediment (Fig. 2B) showed negative $\delta^{13}C$ and $\delta^{18}O$ values with only minor variation between the crystalline filling ($\delta^{13}C = -13.55‰$, $\delta^{18}O = -10.51‰$), the transition zone (mixing bulk sediment and crystalline material, $\delta^{13}C = -15.56‰$, $\delta^{18}O = -10.04‰$) and the bulk sediment matrix ($\delta^{13}C = -13.44‰$, $\delta^{18}O = -8.89‰$). The latter phase was dominated by vaterite ($CaCO_3$).

The crystalline crust on top of bulk sediment (Fig. 2A) showed less negative $\delta^{13}C$ (−0.90‰) and positive $\delta^{18}O$ (3.60‰) values. An additional crystalline vein-like structure, extracted from push corer sediment (Table 3), consisted mainly of aragonite and to a smaller extend of quartz ($Si(O)_2$) reflecting almost identical isotope signatures ($\delta^{13}C = -0.92‰$, $\delta^{18}O = 3.60‰$).

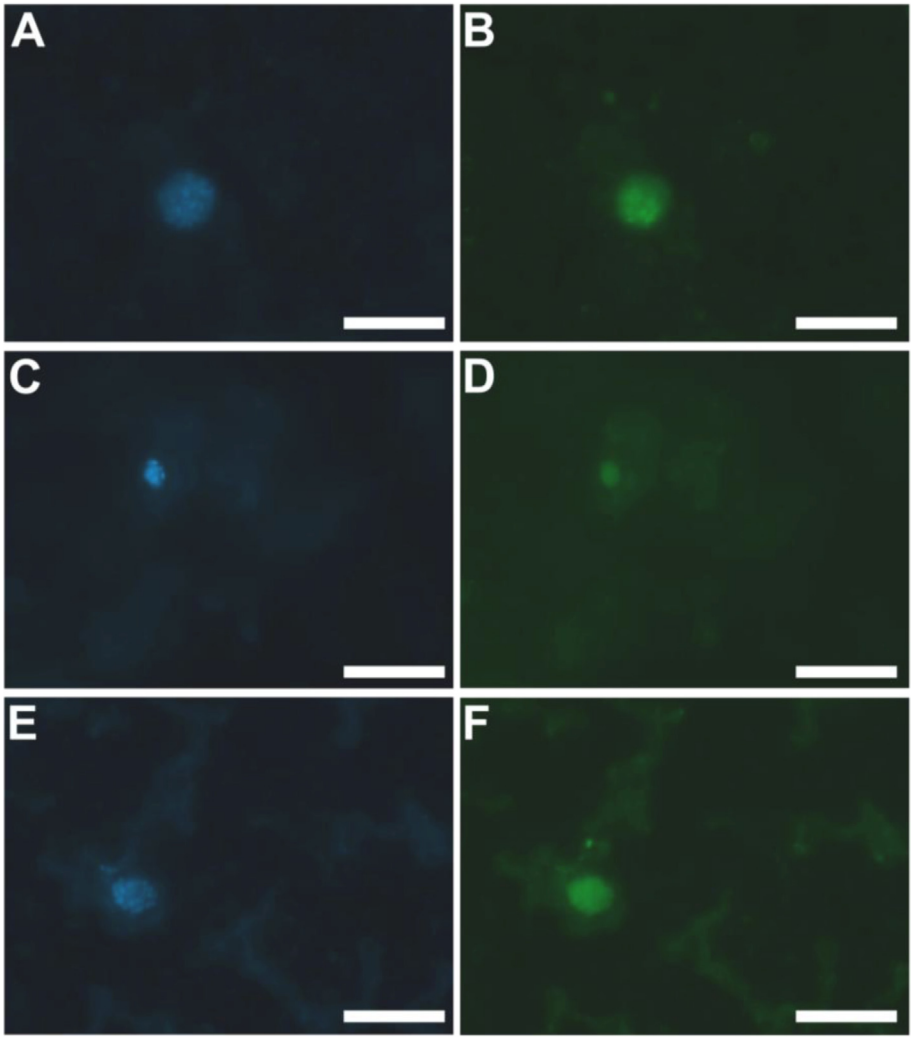

Fig. 6. Epifluorescence images of ANME-2 cells from blowout crater sediments. Cells were stained with DAPI (blue) and CARD-FISH (Alexa 488, green) using probe ANME-2-538. (A, B) ANME-2 cell aggregates from the sediment depth 0–6 cm; (C, D) 6–12 cm; (E, F) 12–18 cm. The scale bar is 10 μm. (For interpretation of the references to color in this figure legend, the reader is referred to the web version of this article.)

3.5. Foraminifera

The living foraminiferal fauna in the blowout crater was dominated by species that are usually infrequent in this part of the North Sea (Table 4). They were otherwise frequent in the deep Norwegian Channel or Norwegian fjords (e.g. *Eggerelloides medius, Labrospira crassimargo, Reophax fusiformis* and *Elphidium incertum*), or dominated the assemblages around the Orkneys and Shetland islands as well as on the Hebrides shelf or around Helgoland (*Trochammina astrifica*, *Textularia earlandi* and *Cibicides lobatulus*) (Küppers, 1987; Murray, 1985, 2003). Benthic foraminifera common in the central middle North Sea and the southern part of the northern North Sea (Murray, 1992; Klitgaard-Kristensen et al., 2002), for instance *Stainforthia fusiformis, Bulimina marginata, Elphidium excavatum* and *Hyalinea balthica* as well as *Cassidulina obtusa*, *Trifarina angulosa* and *Cassidulina leavigata* were either rare or not found in the blowout crater sample. Only the high proportion of *Elphidium excavatum* in the dead assemblage at the blowout is in agreement with literature data from other northern North Sea samples. Surprisingly, *Elphidium incertum* is very frequent in the dead assemblage as well, whereas it is rare in the living fauna. Foraminifera known to recruit elevated objects or hard substrates, i.e. epibenthic species, comprised 78% of the living and 8% of the dead specimens. The proportion of agglutinated species is with 8% of the dead assemblage not substantially higher than in the ambient areas from where proportions of 3–17 % were reported (Jarke, 1961; his map 6). A unique feature was the high abundance of a yet undescribed *Cibicides* species (J. Murray, Southampton, pers. comm.) (Fig. 7). Similar morphotypes have been found in the Celtic Sea (S. Dorst, Kiel, pers. comm.) and off western Iberia (J. Schönfeld, unpubl. data). The stable oxygen composition of *Cibicides lobatulus* from the blowout crater was 1.73‰ and the carbon isotope composition was −0.66‰.

Table 2
Counts of DAPI-stained single cells and cell aggregate (alias ANME-2, see text) at the blowout and the reference site.

Site	Depth (cmbsf)	Single cells (cells cm^{-3})	Aggregate density (aggregates cm^{-3})
Blowout	0–6	7.46×10^8	2.20×10^7
	6–12	4.01×10^8	0.61×10^7
	12–18	4.46×10^8	1.28×10^7
Reference	0–6	7.10×10^8	0
	6–12	3.91×10^8	0
	12–15	7.35×10^8	0

Table 3
Mineral and isotope composition of carbonate samples from the blowout crater. Deviations in the mineral composition to 100 wt.% are caused by the share of pure silicon from the sampling plate, by global amorphous material and by minerals with a share below 5%.

Description	Mineral 1 (wt.%)	Mineral 2 (wt.%)	Mineral 3 (wt.%)	Mineral 4 (wt.%)	Mineral 5 (wt.%)	$\delta^{18}O$	$\delta^{13}C$	Origin
Crystalline structure	Brucite (52)	Calcite (27)	Magnesite (17)	–	–	−10.51	−13.55	Cemented crater sediment/sample extracted from a crack in the bulk sediment/ submersible JAGO
Transition crystalline structure/bulk sediment	Brucite (55)	Calcite (35)	–	–	–	−10.04	−15.56	
Bulk sediment	Vaterite (34)	Calcite (23)	Magnesite (22)	Aragonite (10)	Brucite (7)	−8.89	−13.44	
Crystalline crust on top of bulk sediment	Brucite (48)	Aragonite (38)	Calcite (7)	Magnesite (6)		3.60	−0.90	Cemented crater sediment/top of sediment/ submersible JAGO
Crystalline spheres inside clam shell	Aragonite (80)	–	–		–	4.37	1.49	Cemented crater sediment/extracted from push corer (horizon 6–12 cm bsf)
Crystal vein within bulk sediment	Aragonite (82)	Quartz (11)	–	–	–	3.60	−0.92	
Bulk sediment enclosing crystal vein	–	–	–	–	–	3.95	−0.52	
C. *lobatulus*	–	–	–	–	–	1.73	−0.66	Top 1 cm of crater sediment

Table 4
Living (rose Bengal stained) and dead benthic foraminiferal species >125 μm from the blowout crater and their occurrence in adjacent areas (after Küppers, 1987; Jarke, 1961; Murray, 1985, 1992, 2003, 2006; Klitgaard-Kristensen et al., 2002). Proportion ranges of frequent species in the specific areas are given in brackets. * named *Textularia tenuissima*, ** including other *Rosalina* species.

Sample: Pushcore 36, 0–1 cm	Living fauna (%)	Dead assemblage (%)	Species common in or around		
Species			Norwegian Channel or Skandinavian fjords	Orkneys, Shetlands and Hebrides, Helgoland	Central and northern North Sea
Reophax scorpiurus	4.1	2.1	X		
Eggerelloides medius	2.0	2.1	X (1–49%)	X (6–20%)	
Labrospira crassimargo	3.0	1.4	X (3–11%)		
Reophax fusiformis	0.5	0.7	X (1–5%)		
Textularia earlandi	7.6	0.7		X (4–16%)*	
Trochammina astrifica	5.6	–		X (4–10%)	
Saccammina sphaerica	0.5	1.4			
Stainforthia fusiformis	0.5	0.7	X (28–77%)		X (29–96%)
Bulimina marginata	0.5	1.4		X (4–34%)	X (26–41%)
Trifarina angulosa	–	2.1	X (6–27%)	X (5–18%)	
Cassidulina obtusa	0.5	5.0			
Cassidulina laevigata	–	2.9	X (49–89%)	X (6–19%)	X (7–41%)
Elphidium incertum	1.0	31.4			
Elphidium excavatum	1.0	24.3		X (50%)	X (1–89%)
Hyalinea balthica	0.5	2.1			X (11–24%)
Astrononion stelligerum	0.5	–			
Haynesina orbiculare	0.5	6.4			
Neoconorbina nitida	1.0	–			
Rosalina vilardeboana	1.0	1.4		X (4–58%)**	
Cibicides lobatulus	32.0	3.6		X (13–63%)	
Cibicides sp.	37.6	2.9			
Elphidium excavatum clavatum	–	2.1			
Islandiella islandica	–	1.4			
Quinqueloculina seminula	–	0.7			
Elphidium groenlandicum	–	0.7			
Buccella frigida	–	0.7			
Ammonia batava	–	0.7			
indet. sp.	–	0.7			
Number of counted specimens	197	140			
Sample volume (cm^3):	55	55			
Split	5/8	1/16			
Population density (ind./10 cm^3)	58	419			
Fisher alpha index	5.2	8.9			

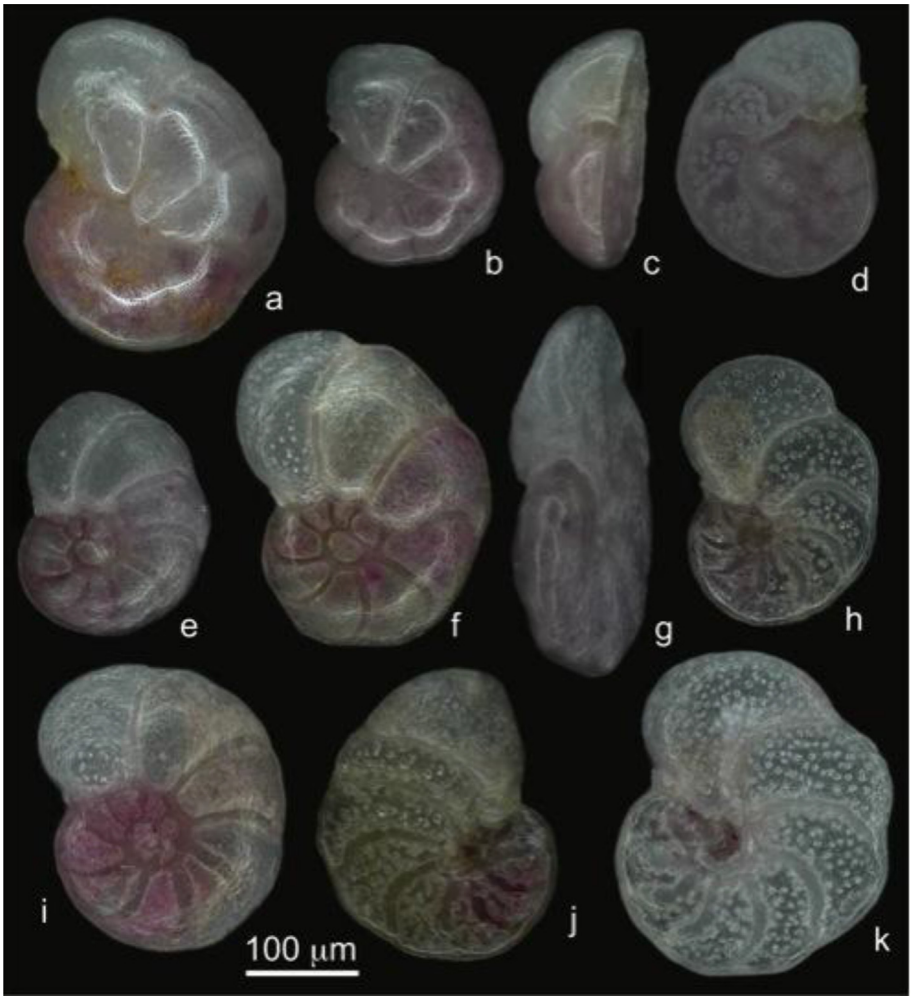

Fig. 7. Living (rose Bengal stained) *Cibicides lobatulus* (a–d) and *Cibicides* sp. (e–k) from sample NF2011-ROV10-PC36, 0–1 cm. Images were taken with a Keyence VHX – 700 FD digital camera at Institute for Geosciences, Kiel University.

4. Discussion

4.1. The magnitude of AOM activity

Potential AOM activity determined in blowout crater sediments in vitro was similar to well-established cold seep habitats, e.g. in the Black Sea or at Hydrate Ridge, but considerably higher compared to natural methane seeps in the North Sea (compare Table 5). AOM rates from the blowout crater determined in intact sediment cores (ex situ) with radiotracer techniques directly after retrieval also reached values (up to 3000 nmol cm^{-3} d^{-1}, L. Steinle, unpubl. data) similar to our study. The agreement between field and potential (in-vitro) turnover rates indicates that in both systems substrates (sulfate and methane) were abundantly available. Most likely, venting methane bubbles enable quick replenishment of sulfate in the sandy, permeable North Sea surface sediments by introducing the convection of seawater during their movement (Treude and Ziebis, 2010). Consequently we expect the AOM zone at the North Sea site to be rather broad compared to cold seeps with low-permeable, fine-grained sediments that hamper quick sulfate replenishment (e.g. Treude et al., 2003; de Beer et al., 2006; Joye et al., 2004; Niemann et al., 2006). Since sulfate concentration was still 25 mM at our maximum sampling depth (15 cmbsf), the AOM zone probably easily extends beyond this depth. Consequently, integrated AOM rates most likely underestimated the total capacity of AOM.

In contrast to the blowout crater, no methane-dependent sulfate reduction or ANME-2 aggregates were found at the reference site, suggesting that the AOM community at the blowout site was established during the past 20 years. However, when the blowout crater was formed, the top 20 m of the surface sediment were removed (Schneider von Deimling et al., in this issue). Hence, we cannot exclude that the blowout uncovered an AOM community, which already existed at 20 mbsf. Nevertheless, it appears rather unlikely that sulfate penetrates 20 m into the seafloor in such a high-productive shelf zone to fuel AOM at this depth (Jørgensen et al., 1990). Additionally, ANME-2 organisms are hypothesized to occur mainly in surface-near sediments (top 10 cm) of cold seeps (Knittel and Boetius, 2009 and references therein).

4.2. Formation of methane-related carbonates

Considering the magnitude of AOM rates at the blowout site, MDAC formation would generally be feasible within 20 years (Luff et al., 2004). However, based on isotope analyzes we could not find any indications for MDAC formation in blowout crater sediments. In some samples aragonite and magnesite, common MDAC (Ritger et al., 1987; Greinert and Derkachev, 2004), were found.

Table 5
Comparison of AOM rates at different methane habitats.

Sampling site	Range of AOM rates (nmol cm^{-3} d^{-1})	Integrated (mmol m^{-2} d^{-1})	Rate determination	References
Cold seep (methanotrophic reefs) Black Sea	1000–10,000	–	Potential/in vitro	Treude et al., 2007
Cold seep (Hydrate Ridge) Pacific Ocean	200–5500	5–99	Potential/in vitro & ex situ	Treude et al., 2003; Boetius et al., 2000
Cold seep (Santa Barbara Channel) Pacific Ocean	10–280	0.6–8.7	ex situ	Treude and Ziebis 2010
Cold seep (Green Canyon area) Gulf of Mexico	100–500	1–13	ex situ	Joye et al., 2004
Mud volcano (Håkon-Mosby) Atlanic Ocean	10–500	12–19	ex situ	Niemann et al., 2006
Gas seep (Blowout), North Sea	540–2800	200–375	Potential/in vitro	This study
Organic rich sediments (Eckernförde Bay) Baltic Sea	5–18	0.9–1.5	Potential/in vitro & ex situ	Treude et al., 2005
Cold seep (Gullfaks & Tommeliten) North Sea	2–90	13	Potential/in vitro & ex situ	Niemann et al., 2005; Wegener et al., 2008

Some samples were depleted in ^{13}C isotopes, which could indicate that mineral formation was influenced by AOM. However, corresponding $\delta^{18}O$ values were strongly negative. In fact, measured $\delta^{18}O$ values ranging from −8.81 to −10.51‰ indicate that mineral genesis took place at temperatures considerably higher than encountered in the marine realm during Phanerozoic (Veizer, 1999). Consequently, these samples do not represent pristine marine authigenic carbonates.

MDAC formed under present day conditions, showed always positive $\delta^{18}O$ values (Hovland et al., 1987; Bohrmann et al., 1998; Naehr et al., 2007). Furthermore, total alkalinity in crater sediments was almost one order of magnitude lower compared to other cold seeps with similar AOM activity and substantial MDAC formation (Luff and Wallmann, 2003; Lein, 2004; Boetius et al., 2009). We suggest that MDAC formation is either inhibited or retarded in the surface sediments of the blowout site, because permeable sediments in combination with upward streams of gas and fluids facilitate quick removal of bicarbonate, thereby preventing an increase in total alkalinity in the porewater and consequently carbonate formation (Luff et al., 2004). In summary, the mineralogical and isotope geochemical investigation of small-scale incrustation and carbonate coatings did not reveal evidence for MDAC formation on the crater bottom.

4.3. Foraminiferal assemblage composition and isotopic signatures

The benthic foraminiferal assemblage composition in the blowout crater revealed that this fauna was unique to the blowout site and thus characterized an environment distinctively different to other areas of the North Sea (Jarke, 1961; Murray, 1992; Klitgaard-Kristensen et al., 2002). The high proportion of epibenthic species indicated that lateral advection of food particles by near-bottom turbulences or currents was the dominating environmental factor for the foraminiferal assemblages in the blowout crater (Lutze and Thiel, 1989; Schönfeld, 2002; Nauw et al., in this issue; Schneider von Deimling et al., in this issue). The underrepresentation of the epibenthic *Cibicides lobatulus* and *Cibicides* sp. in the dead assemblage is most likely due to the high turbulences in the crater. The empty, lightweight foraminiferal tests were kept in suspension and could be easily transported out of the crater. A similar long-distance transport of light epibenthic foraminifera in turbulence has been described from the Gulf of Cadiz, Spain (Rogerson et al., 2011). Likewise, the large and robust tests of *Elphidium incertum* could be enriched in the dead fauna. A contribution of re-deposited foraminiferal tests from the eroded glacial clays of the crater wall are considered as less significant, because the arctic species *Buccella frigida, Islandiella islandica*, and *Elphidium groenlandicum* are rare in the dead assemblage. The stable isotope analyzes of calcareous, epibenthic *Cibicides lobatulus* nonethe-less indicate the influence of methane-related carbon. Oxygen and carbon isotopes are incorporated in their tests in equilibrium to ambient seawater with an offset due to vital effects. The species-specific offset of *C. lobatulus* carbon isotopes with reference to ambient seawater, i.e. the so-called vital effect, has been constrained to +0.4‰ in $\delta^{13}C$ (Mackensen et al., 2001; Owen et al., 2002; Scourse et al., 2004). For the North Sea, sparse information exists about $\delta^{13}C$ of seawater dissolved inorganic carbon ($\delta^{13}C_{DIC}$). Values range between +0.3 and +0.6‰ (Hellings et al., 1999; Ahad et al., 2008; Brückner and Mackensen, 2008). Assuming a $\delta^{13}C_{DIC}$ at the blowout of +0.4‰ would give a $\delta^{13}C$ value for *C. lobatulus* of +0.8‰. The measured $\delta^{13}C$ value of −0.66‰ is, however, lower by 1.46‰. Even though this difference is not supported by replicate analyses, the offset is substantial, and is justified to be attributed to the influence of carbon derived from AOM or by isotopically light formation water from greater depths. However, the $\delta^{13}C_{DIC}$ of seawater or sediment porewater in the blowhole has not been measured yet to further constrain these contentions. The strong $\delta^{13}C$ offset between epibenthic foraminifera and ambient seawater depicted the UK22/4b blowout as the second site worldwide after Håkon-Mosby mud volcano (Mackensen et al., 2006), where a marked influence of isotopically light CO_2 on the biomineralization of benthic organisms has been recorded. Benthic foraminifera are not primarily involved in methane turnover. As such, methane seepage at the blowout exerts an influence on biogeochemical processes beyond the inter-relationships within certain food chains. Evidences for this impact are potentially deliverable to the fossil record conveyed by foraminiferal shells (Panieri et al., 2009). The pervasive environmental impact of the blowout is clearly mirrored in the foraminiferal assemblage composition. Hence, it is justified to conclude that living benthic communities might be a far more sensitive indicators for recent environmental changes induced by enhanced AOM than their biomineralization products.

4.4. Adaptation of AOM to methane fluxes and implications for future emission scenarios

Modeling approaches demonstrated that the establishment of a steady-state AOM biomass in response to an onset of methane flux would take approximately 60 years (Dale et al., 2008). In comparison to our study site, methane flux in this numerical simulation was rather slow. After 12 years, methane reaches the sediment–water interface. Then, after an additional 13 years, the AOM zone

becomes established. From then on, the model predicts a log growth phase. Providing that in our scenario methane and sulfate were available from the first day of the blowout accident, exponential growth phase of AOM organisms could start immediately. Hence, the presence of a highly active AOM community at the blowout site after only 20 years does not necessarily contradict the simulations of Dale et al. (2008).

The adaptation potential of the benthic microbial methane filter is of interest especially considering the fate of methane emitted from dissociating methane hydrates affected by future Global Warming. Rates, time scales, and the extent to which hydrates will destabilize in such scenarios are still under debate (Archer, 2007; Brook et al., 2008; Biastoch et al., 2011). Evaluation of the capacity of the benthic microbial methane filter to retain methane in response to such events appears even more difficult. Our data indicate that high concentrations of AOM biomass can establish in initially "pristine" sediments at most within two decades after seepage initiation. This observation confirms earlier studies of in-vitro growth in non-seep sediments (Girguis et al., 2005) and from deep-sea whale falls (Goffredi et al., 2008), where AOM organisms appeared within months to a few years, respectively, after methane became available in the sediment.

At the shallow blowout site, high sediment permeability combined with vigorous gas emissions most likely creates a broad SMTZ for capturing methane. However, without the formation of carbonates, no long-term sink for methane-derived carbon is provided. Methane hydrates, on the other hand, are features of continental slopes, which are often characterized by less permeable, fine-grained sediments. Here, diffusion limitation leads to a shallower penetration of sulfate under high methane consumption (Treude, 2003), and hence limits AOM activity and methane removal to a relatively narrow horizon thereby enhancing the potential to increase alkalinity in the porewater and to store methane-derived carbon in the form of carbonates. It is therefore problematic to put mechanisms controlling the benthic methane filter at the shallow blowout site on the same level as areas of gas hydrate dissociation on continental slopes.

Ultimately, the efficiency of the benthic methane filter will depend on type and velocity of methane transport and the availability of electron acceptors. Given the vigorous release of gaseous methane from the sediments at the blowout site, we expect the relative amount of benthic microbial consumption to be rather small. In order to test this hypothesis, deeper coring would be necessary to reveal the full extent and capacity of AOM.

5. Conclusion

The UK22/4b blowout in the northern North Sea represents a model site to study the effect of a sudden onset of methane releases on benthic biogeochemical processes. We demonstrated that a very active anaerobic methanotrophic community established within at least two decades. Furthermore, we discovered that the methane seepage affected the carbon isotopic signature of epibenthic foraminifera and the community structure of foraminiferal assemblages that are not participating in the methane carbon food chain. Given the permeable nature of the sandy sediments at the investigated sites, we conclude that massive methane-derived authigenic carbonates were unable to form in the surface sediments within the given time span, because continuous exchange of porewater, driven by the vigorous gas discharge, most likely retards the build up of carbonate alkalinity within the crater structure itself. Together, these observations might provide a useful new tool to identify strong shallow methane seeps in the geological record or to predict related biogeochemical reactions in numerical simulations.

Acknowledgments

We thank B. Domeyer, A. Bleyer and M. Dibbern for pore water analyzes. Additionally, we acknowledge J. Heinze and N. Augustin for technical support during XRD analyzes as well as L. Haxhiaj for technical support during stable isotope measurements. We thank the Institute for Polar Ecology and Institute for Geosciences, Kiel University, for providing their microscopy facilities. Finally, we would like to thank the crew and all scientists who helped during the cruises with R/V ALKOR, NOORDHOEK PATHFINDER (funding by DECC/ExxonMobil) and R/V CELTIC EXPLORER (funding by EUROFLEETS) and the team of the submersible JAGO. This research was part of the Excellence Cluster "The Future Ocean" funded by the German Research Foundation (DFG).

References

Ahad, J.M.E., Barth, J.A.C., Ganeshram, R.S., Spencer, R.G.M., Uher, G., 2008. Controls on carbon cycling in two contrasting temperate zone estuaries: the Tyne and Tweed, UK. Estuar. Coast. Shelf Sci. 78 (4), 685–693.

Aloisi, G., Bouloubassi, I., Heijs, S.K., Pancost, R.D., Pierre, C., Sinninghe, D.J.S., et al., 2002. CH_4-consuming microorganisms and the formation of carbonate crusts at cold seeps. Earth Planet. Sci. Lett. 203 (1), 195–203.

Amann, R.I., Binder, B.J., Olson, R.J., Chrisholm, S.W., Devereux, R., Stahl, D.A., 1990. Combination of 16S ribosomal-RNA-targeted oligonucleotide probes with flow-cytometry for analyzing mixed microbial-populations. Appl. Environ. Microbiol. 56 (6), 1919–1925.

Archer, D., 2007. Methane hydrate stability and anthropogenic climate change. Biogeosciences 4 (4), 521–544.

Barnes, R.O., Goldberg, E.D., 1976. Methane production and consumption in anoxic marine sediments. Geology 4 (5), 297.

Bayon, G., Henderson, G.M., Bohn, M., 2009. U–Th stratigraphy of a cold seep carbonate crust. Chem. Geol. 260, 47–56.

de Beer, D., Sauter, E., Niemann, H., Kaul, N., Foucher, J.P., Witte, U., et al., 2006. In situ fluxes and zonation of microbial activity in surface sediments of the Hakon Mosby Mud Volcano. Limnol. Oceanogr. 51 (3), 1315–1331.

Biastoch, A., Treude, T., Rüpke, L.H., Riebesell, U., Roth, C., Burwicz, E.B., Park, W., Latif, M., Böhning, C.W., Madec, G., Wallmann, K., 2011. Rising Arctic Ocean temperatures cause gas hydrate destabilization and ocean acidification. Geophys. Res. Let. 38.

Boetius, A., Holler, T., Knittel, K., Felden, J., Wenzhöfer, F., 2009. The seabed as natural laboratory: lessons from uncultivated methanotrophs. In: Epstein, S.S. (Ed.), Microbiology Monographs. Springer Berlin Heidelberg, Berlin, Heidelberg, pp. 59–82.

Boetius, A., Ravenschlag, K., Schubert, C.J., Rickert, D., Widdel, F., Gieseke, A., Amann, R., Jørgensen, B.B., Witte, U., Pfannkuche, O., 2000. A marine microbial consortium apparently mediating anaerobic oxidation of methane. Nature 407 (6804), 623–626.

Bohrmann, G., Greinert, J., Suess, E., Torres, M., 1998. Authigenic carbonates from the Cascadia subduction zone and their relation to gas hydrate stability. Geology 26 (7), 647.

Brook, E., Archer, D., Dlugokencky, E., Frolking, S., Lawrence, D., 2008. Chapter 5: potential for abrupt changes in atmospheric methane. Abrupt Climate Change. A Report by the U.S. Climate Change Science Program, U.S. Geological Survey: Reston, vol. 2008, pp. 163–201.

Brückner, S., Mackensen, A., 2008. Organic matter rain rates, oxygen availability, and vital effects from benthic foraminiferal $\delta^{13}C$ in the historic Skagerrak, North Sea. Mar. Micropaleontol. 66 (3–4), 192–207.

Cord-Ruwisch, R., 1985. A quick method for the determination of dissolved and precipitated sulfides in cultures of sulfate-reducing bacteria. J. Microbiol. Meth. 4, 33–36.

Dale, A.W., van Cappellen, P., Aguilera, D.R., Regnier, P., 2008. Methane efflux from marine sediments in passive and active margins: estimations from bioenergetic reaction–transport simulations. Earth Planet. Sci. Let. 265 (3–4), 329–344.

Girguis, P.R., Cozen, A.E., DeLong, E.F., 2005. Growth and population dynamics of anaerobic methane-oxidizing archaea and sulfate-reducing bacteria in a continuous-flow bioreactor. Appl. Environ. Microbiol. 71 (7), 3725–3733.

Goffredi, S.K., Wilpiszeski, R., Lee, R., Orphan, V., 2008. Temporal evolution of methane cycling and phylogenetic diversity of archaea in sediments from a deep-sea whale-fall in Monterey Canyon, California. ISME J. 2, 204–220.

Greinert, J., Bohrmann, G., Suess, E., 2001. Gas hydrate-associated carbonates and methane-venting at Hydrate Ridge: classification, distribution, and origin of authigenic lithologies. Geophys. Monogr. Ser. 124, 99–113.

Greinert, J., Derkachev, A., 2004. Glendonites and methane-derived Mg-calcites in the Sea of Okhotsk, Eastern Siberia: implications of a venting-related ikaite/glendonite formation. Mar. Geol. 204 (1–2), 129–144.

Haffert, L., Haeckel, M., Liebetrau, V., Berndt, C., Hensen, C., Nuzzo, M., Reitz, A., Scholz, F., Schönfeld, J., Perez-Garciac, C., Weise, S.M., 2013. Fluid evolution and authigenic mineral paragenesis related to salt diapirism – the Mercator mud volcano in the Gulf of Cadiz. Geochim. Cosmochim. Acta 106, 261–286.

Hein, J.R., Normark, W.R., McIntyre, B.R., Lorenson, T.D., Powell II, C.L., 2006. Methanogenic calcite, ^{13}C-depleted bivalve shells, and gas hydrate from a mud volcano offshore southern California. Geololgy 34, 109–112.
Hellings, L., Dehairs, F., Tackx, M., Keppens, E., Baeyens, W., 1999. Origin and fate of organic carbon in the freshwater part of the Scheldt estuary as traced by stable carbon isotope composition. Biogeochemistry 47 (2), 167–186.
Hill, T.M., Kennett, J.P., Valentine, D.L., 2004. Isotopic evidence for the incorporation of methane-derived carbon into foraminifera from modern methane seeps, Hydrate Ridge, Northeast Pacific. Geochim. Cosmochim. Acta 68 (22), 4619–4627.
Hovland, M., Talbot, M.R., Qvale, H., Olaussen, S., Aasberg, L., 1987. Methane-related carbonate cements in pockmarks of the North Sea. J. Sed. Petrol 57 (5), 881–892.
Hungate, R.E., 1950. The anaerobic mesophilic cellulolytic bacteria. Bacteriol. Rev. 14, 0–49.
IPCC, 2007. The Scientific Basis. Contribution of Working Group I to the Fourth Assessment Report of the Intergovernmental Panel on Climate Change (IPCC). Cambridge University Press, Cambridge, MA.
Ivanenkov, V.N., Lyakhin, V.N., 1978. Determination of total alkalinity in seawater. In: Bordovsky, O.K., Ivanenkov, V.N. (Eds.), Methods of Hydrochemical Investigations in the Ocean. Nauka Publ. House, Moscow, pp. 110–114.
Jarke, J., 1961. Die Beziehungen zwischen hydrographischen Verhältnissen, Faziesentwicklung und Foraminiferenverbreitung in der heutigen Nordsee als Vorbild für die Verhältnisse während der Miozän-Zeit. Meyniana 10, 21–36.
Jørgensen, B.B., Bang, M., Blackburn, T.H., 1990. Anaerobic mineralization in marine sediments from the Baltic Sea-North Sea transition. Mar. Ecol. Prog. Ser. 59, 39–54.
Joye, S.B., Boetius, A., Orcutt, B.N., Montoya, J.P., Schulz, H.N., Erickson, M.J., Lugo, S.K., 2004. The anaerobic oxidation of methane and sulfate reduction in sediments from Gulf of Mexico cold seeps. Chem. Geol. 205 (3–4), 219–238.
Kallmeyer, J., Ferdelman, T.G., Weber, A., Fossing, H., Jørgensen, B.B., 2004. Evaluation of a cold chromium distillation procedure for recovering very small amounts of radiolabeled sulfide related to sulfate reduction measurements. Limnol. Ocean. Meth. 2, 171–180.
Klitgaard-Kristensen, D., Sejrup, H.F., Haflidason, H., 2002. Distribution of recent calcareous benthic foraminifera in the northern North Sea and relation to the environment. Polar Res. 21 (2), 275–282.
Knittel, K., Boetius, A., 2009. Anaerobic oxidation of methane: progress with an unknown process. Annu. Rev. Microbiol. 63 (1), 311–334.
Knittel, K., Lösekann, T., Boetius, A., Kort, R., Amann, R., 2005. Diversity and distribution of methanotrophic archaea at cold seeps. Appl. Environ. Microbiol. 71 (1), 467–479.
Krause, S., Steeb, P., Hensen, C., Liebetrau, V., Dale, A.W., Nuzzo, M., Treude, T., 2013. Microbial activity and carbonate isotope signatures as a tool for identification of spatial differences in methane advection: a case study at the Pacific Costa Rican margin. Biogeosci. Disc. 10 (5), 8159–8201.
Küppers, R., 1987. Systematische und ökologische Studien zur Bestandsaufnahme der Foraminiferenfauna um Helgoland in Abhängigkeit vom Jahresgang. Rheinische Friedrich-Wilhelms Universität, Bonn, p. 361.
Leifer, I., Solomon, E., Schneider von Deimling, J., Rehder, G., Coffin, R., Linke, P., 2015. The fate of bubbles in a large, intense bubble megaplume for stratified and unstratified water: numerical simulations of 22/4b expedition field data. J. Mar. Petrol. Geol. (in this issue).
Leifer, I., Judd, A., 2015. The UK22/4b blowout 20 years on: investigations of continuing methane emissions from sub-seabed to the atmosphere in a North Sea Context. J. Mar. Petrol. Geol. (in this issue).
Lein, A.Y., 2004. Authigenic carbonate formation in the ocean. Lithol. Mineral. Resour. 39 (1), 3–35.
Liebetrau, V., Eisenhauer, A., Linke, P., 2010. Cold seep carbonates and associated cold-water corals at the Hikurangi Margin, New Zealand: new insights into fluid pathways, growth structures and geochronology. Mar. Geol. 272 (1–4), 307–318.
Linke, P. (Ed.), 2012. RV Celtic Explorer EUROFLEETS cruise reportCE12010-ECO2@NorthSea, 20.07.-06.08.2012, Bremerhaven-Hamburg. GEOMAR-Report, N. Ser.004. Kiel, 60 pp. doi:10.3289/GEOMAR_REP_NS_4_2012.
Lösekann, T., Knittel, K., Nadalig, T., Fuchs, B., Niemann, H., Boetius, A., Amann, R., 2007. Diversity and abundance of aerobic and anaerobic methane oxidizers at the Haakon Mosby mud volcano, Barents Sea. Appl. Environ. Microbiol. 73 (10), 3348–3362.
Luff, R., Wallmann, K., 2003. Fluid flow, methane fluxes, carbonate precipitation and biogeochemical turnover in gas hydrate-bearing sediments at Hydrate Ridge, Cascadia Margin: numerical modeling and mass balances. Geochim. Cosmochim. Acta 67 (18), 3403–3421.
Luff, R., Wallmann, K., Aloisi, G., 2004. Numerical modeling of carbonate crust formation at cold vent sites: significance for fluid and methane budgets and chemosynthetic biological communities. Earth Planet. Sci. Lett. 221 (1–4), 337–353.
Lutze, G.-F., Thiel, H., 1989. Epibenthic foraminifera from elevated microhabitats: *Cibicidoides wuellerstorfi* and *Planulina ariminensis*. J. Foram. Res. 19, 153–158.
Mackensen, A., Schumacher, S., Radke, J., Schmidt, D.N., 2001. Microhabitat preferences and stable carbon isotopes of endobenthic foraminifera: clue to quantitative reconstruction of new production? Mar. Micropaleontol. 40, 233–258.
Mackensen, A., Wollenburg, J., Licari, L., 2006. Low d^{13}C in tests of live epibenthic and endobenthic foraminifera at a site of active methane seepage. Paleoceanography 21.
McConnaughey, T.A., Burdett, J., Whelan, J.F., Paull, C.K., 1997. Carbon isotopes in biological carbonates: respiration and photosynthesis. Geochim. Cosmochim. Acta 61, 611–622.
Milucka, J., Ferdelman, T.G., Polerecky, L., Franzke, D., Wegener, G., Schmid, M., Lieberwirth, I., Wagner, M., Widdel, F., Kuypers, M.M.M., 2012. Zero-valent sulphur is a key intermediate in marine methane oxidation. Nature 491, 541–546.
Murray, J.W., 1985. Recent foraminifera from the North Sea (Forties and Ekofisk areas) and the continental shelf west of Scotland. J. Micropalaeontol. 4, 117–125.
Murray, J.W., 1992. Distribution and population dynamics of benthic foraminifera from the southern North Sea. J. Foraminifer. Res. 22, 114–128.
Murray, J.W., 2003. An illustrated guide to the benthic foraminifera of the Hebridean shelf, west of Scotland, with notes on their mode of life. Palaeontol. Electron. 5 (2), 1–31.
Murray, J.W., 2006. Ecology and Applications of Benthic Foraminifera. Cambridge University Press, p. 426.
Naehr, T.H., Eichhubl, P., Orphan, V.J., Hovland, M., Paull, C.K., Ussler, W., et al., 2007. Authigenic carbonate formation at hydrocarbon seeps in continental margin sediments: a comparative study. Deep Sea Res. II Top. Stud. Oceanogr. 54 (11–13), 1268–1291.
Nauw, J., Linke, P., Leifer, I., 2015. Bubble momentum plume as a possible mechanism for an early breakdown of the seasonal stratification in the northern North Sea. J. Mar. Petrol. Geol. (in this issue).
Nauhaus, K., Boetius, A., Kruger, M., Widdel, F., 2002. In vitro demonstration of anaerobic oxidation of methane coupled to sulphate reduction in sediment from a marine gas hydrate area. Environ. Microbiol. 4 (5), 296–305.
Niemann, H., Elvert, M., Hovland, M., Orcutt, B., Judd, A., Suck, I., Gutt, J., Joye, S.B., Damm, E., Finster, K., Boetius, A., 2005. Methane emission and consumption at a North Sea gas seep (Tommeliten area). Biogeosciences 2 (4), 335–351.
Niemann, H., Lösekann, T., Beer, D., Elvert, M., Nadalig, T., Knittel, K., Aman, A., Sauter, E.J., Schlüter, M., Klages, M., Foucher, J.-P., Boetius, A., 2006. Novel microbial communities of the Haakon Mosby mud volcano and their role as a methane sink. Nature 443, 854–858.
Orphan, V.J., House, C.H., Hinrichs, K.U., McKeegan, K.D., DeLong, E.F., 2001. Methane-consuming archaea revealed by directly coupled isotopic and phylogenetic analysis. Science 293, 484–487.
Owen, R., Kennedy, H., Richardson, C., 2002. Isotopic partitioning between scallop shell calcite and seawater: effect of shell growth rate. Geochim. Cosmochim. Acta 66 (10), 1727–1737.
Panieri, G., 2006. Foraminiferal response to an active methane seep environment: a case study from the Adriatic Sea. Mar. Micropaleontol. 61, 116–130.
Panieri, G., Camerlenghi, A., Conti, S., Pini, G.A., Cacho, I., 2009. Methane seepages recorded in benthic foraminifera from Miocene seep carbonates, Northern Apennines (Italy). Palaeogeogr. Palaeoclimatol. Palaeoecol. 284 (3–4), 271–282.
Peckmann, J., Reimer, A., Luth, U., Luth, C., Hansen, B.T., Heinicke, C., Hoefs, J., Reitner, J., 2001. Methane-derived carbonates and authigenic pyrite from the northwestern Black Sea. Mar. Geol. 177 (1–2), 129–150.
Peckmann, J., Thiel, V., Michaelis, W., Clari, P., Gaillard, C., Martire, L., Reitner, J., 1999. Cold seep deposits of Beauvoisin (Oxfordian; southeastern France) and Marmorito (Miocene; northern Italy. Microbially induced authigenic carbonates. Intern. J. Earth Sci. 88 (1), 60–75.
Pernthaler, A., Pernthaler, J., Amann, R., 2002. Fluorescence in situ hybridization and catalyzed reporter deposition for the identification of marine bacteria. Appl. Environ. Microbiol. 68 (6), 3094–3101.
Rathburn, A.E., Levin, Lisa A., Held, Zachary, Lohmann, K.C., 2000. Benthic foraminifera associated with cold methane seeps on the northern California margin: ecology and stable isotopic composition. Mar. Micropaleontol. 38 (3–4), 247–266.
Rathburn, A.E., Pérez, M.E., Martin, J.B., Day, S.A., Mahn, C., Gieskes, J., Ziebis, W., Williams, D., Bahls, A., 2003. Relationships between the distribution and stable isotopic composition of living benthic foraminifera and cold methane seep biogeochemistry in Monterey Bay, California. Geochem. Geophys. Geosyst. 4 (12), 1106. http://dx.doi.org/10.1029/2003GC000595.
Rehder, G., Keir, R.S., Suess, E., Pohlmann, T., 1998. The multiple sources and patterns of methane in North Sea waters. Aquat. Geochem 4 (3/4), 403–427.
Ritger, S., Carson, B., Suess, E., 1987. Methane-derived authigenic carbonates formed by subduction induced pore-water expulsion along the Oregon Washington Margin. Geol. Soc. Am. Bull. 98 (2), 147–156.
Rogerson, M., Schönfeld, J., Leng, M.J., 2011. Qualitative and quantitative approaches in palaeohydrography: a case study from core-top parameters in the Gulf of Cadiz. Mar. Geol. 280, 150–167.
Schneider von Deimling, J., Brockhoff, J., Greinert, J., 2007. Flare imaging with multibeam systems: data processing for bubble detection at seeps. Geochem. Geophys. Geosyst 8 (6). http://dx.doi.org/10.1029/2007GC001577.
Schneider von Deimling, J., Linke, P., Schmidt, M., Rehder, G., 2015. Ongoing methane discharge at well site 22/4b (North Sea) and discovery of a spiral vortex bubble plume motion. J. Mar. Petrol. Geol. (in this issue).
Schoell, M., 1988. Multiple origins of methane in the Earth. Chem. Geol. 71 (1–3), 1–10.
Schönfeld, J., 2002. A new benthic foraminiferal proxy for near-bottom current velocities in the Gulf of Cadiz, northeastern Atlantic Ocean. Deep Sea Res. I 49, 1853–1875.
Schönfeld, J., Alve, E., Geslin, E., Jorissen, F., Korsun, S., Spezzaferri, S., 2012. The FOBIMO (FOraminiferal BIo-MOnitoring) initiative—Towards a standardised protocol for soft-bottom benthic foraminiferal monitoring studies. Mar. Micropaleontol. 94–95, 1–13.
Scourse, J.D., Kennedy, H., Scott, G.A., Austin, W.E.N., 2004. Stable isotopic analyses of modern benthic foraminifera from seasonally stratified shelf seas: disequilibria and the 'seasonal effect'. Holocene 14 (5), 747–758 .

Sommer, S., Linke, P., Pfannkuche, O., Niemann, H., Treude, T., 2010. Benthic respiration in a seep habitat dominated by dense beds of ampharetid polychaetes at the Hikurangi Margin (New Zealand). Mar. Geol. 272 (1–4), 223–232.

Stott, L.D., Bunn, T., Prokopenko, M., Mahn, C., Gieskes, J., Bernhard, J.M., 2002. Does the oxidation of methane leave an isotopic fingerprint in the geologic record? Geochem. Geophys. Geosyst 3 (2).

Teichert, B.M.A., Eisenhauer, A., Bohrmann, G., Haase-Schramm, A., Bock, B., Linke, P., 2003. U/Th systematics and ages of authigenic carbonates from Hydrate Ridge, Cascadia Margin: recorders of fluid flow variations. Geochim. Cosmochim. Acta 67 (20), 3845–3857.

Thiel, V., Peckmann, J., Richnow, H.H., Luth, U., Reitner, J., Michaelis, W., 2001. Molecular signals for anaerobic methane oxidation in Black Sea seep carbonates and a microbial mat. Mar. Chem. 73 (2), 97–112.

Torres, M.E., 2003. Is methane venting at the seafloor recorded by $\delta^{13}C$ of benthic foraminifera shells? Paleoceanography 18 (3).

Treude, T., 2003. Anaerobic Oxidation of Methane in Marine Sediments. Universität Bremen, Fachbereich Biologie/Chemie, p. 245.

Treude, T., Boetius, A., Knittel, K., Wallmann, K., Jørgensen, B.B., 2003. Anaerobic oxidation of methane above gas hydrates at Hydrate Ridge, NE Pacific Ocean. Mar. Ecol. Prog. Ser. 264, 1–14.

Treude, T., Knittel, K., Blumenberg, M., Seifert, R., Boetius, A., 2005a. Subsurface microbial methanotrophic mats in the Black Sea. Appl. Environ. Microbiol. 71 (10), 6375–6378.

Treude, T., Krüger, M., Boetius, A., Jørgensen, B.B., 2005b. Environmental control on anaerobic oxidation of methane in the gassy sediments of Eckernforde Bay (German Baltic). Limnol. Oceanogr. 50 (6), 1771–1786.

Treude, T., Niggemann, J., Kallmeyer, J., Wintersteller, P., Schubert, C.J., Boetius, A., Jørgensen, B.B., 2005c. Anaerobic oxidation of methane and sulfate reduction along the Chilean continental margin. Geochim. Cosmochim. Acta 69 (11), 2767–2779.

Treude, T., Orphan, V., Knittel, K., Gieseke, A., House, C.H., Boetius, A., 2007. Consumption of methane and CO_2 by methanotrophic microbial mats from Gas Seeps of the anoxic Black Sea. Appl. Environ. Microbiol. 73 (7), 2271–2283.

Treude, T., Ziebis, W., 2010. Methane oxidation in permeable sediments at hydrocarbon seeps in the Santa Barbara Channel, California. Biogeosciences 7 (10), 3095–3108.

Veizer, J., 1999. $^{87}Sr/^{86}Sr$, $\delta^{13}C$ and $\delta^{18}O$ evolution of phanerozoic seawater. Chem. Geol. 161, 17–59.

Wegener, G., Shovitri, M., Knittel, K., Niemann, H., Hovland, M., Boetius, A., 2008. Biogeochemical processes and microbial diversity of the Gullfaks and Tommeliten methane seeps (Northern North Sea). Biogeosciences 5, 1127–1144.

Widdel, F., Bak, F., 1992. Gram-negative mesophilic sulfate-reducing bacteria. In: Balows, A., Trüper, H.G., Dworking, M., Harder, W., Schleifer, K.-H. (Eds.), The Prokaryotes. Springer, New York, pp. 3352–3378.